Narrowband tunable filter based on velocity-selective optical pumping in an atomic vapor

Alessandro Cerè,[1,*] Valentina Parigi,[2] Marta Abad,[1,3] Florian Wolfgramm,[1] Ana Predojević,[1] and Morgan W. Mitchell[1]

[1]ICFO–Institut de Ciencies Fotoniques, Mediterranean Technology Park, 08860 Castelldefels (Barcelona), Spain
[2]LENS, Via Nello Carrara 1, 50019 Sesto Fiorentino, Florence, Italy
[3]Current address: Departament d'Estructura i Constituents de la Matèria, Facultat de Física, Universitat de Barcelona, Diagonal 647, 08028 Barcelona, Spain
*Corresponding author: alessandro.cere@icfo.es

Received December 11, 2008; revised February 18, 2009; accepted February 19, 2009; posted February 25, 2009 (Doc. ID 105202); published March 24, 2009

We demonstrate a tunable narrowband filter based on optical-pumping-induced circular dichroism in rubidium vapor. The filter achieves a peak transmission of 14.6%, a linewidth of 80 MHz, and an out-of-band extinction of ⩾35 dB. The transmission peak can be tuned within the range of the Doppler linewidth of the D_1 line of atomic rubidium at 795 nm. While other atomic filters work at frequencies far from absorption, the presented technique provides light resonant with atomic media, useful for atom–photon interaction experiments. The technique could readily be extended to other alkali atoms. © 2009 Optical Society of America

OCIS codes: 120.2440, 260.3160, 300.6210.

Narrowband optical filters are a necessary resource in many applications where the signal-to-noise ratio is a critical parameter. Applications, such as free space laser communication [1], lidar [2,3], and the generation of narrowband quantum light [4–6], require, together with a high peak transmission, a high out-of-band rejection and frequency stability. Atomic optical filters based on circular birefringence [7–9] have proven to provide a high out-of-band rejection and a practicality of use [2,3]. Other commonly used narrow bandwidth filters are optical cavities. These can attain high transmission efficiency, narrow bandwidth, and frequency tuning. Because of their comb-like transmission spectrum, it is often necessary to use a sequence of two or more cavities with different free spectral ranges [4].

In this Letter we present the realization of an atomic filter based on a circular dichroism in rubidium. The velocity selective pumping permits the tuning of the filter over the range of the Doppler width of the atomic transition [8]. In contrast to birefringence-based filters, ours uses atomic absorption; thus it can be tuned precisely to resonance with the ground-state transitions, a feature particularly desirable in atomic physics experiments, such as stopped light [10]. The design was inspired by the "interaction-free measurement" scheme proposed by Elitzur and Vaidman [11]. Their proposal describes a Mach–Zehnder interferometer with the paths balanced so that one output port is dark. The presence of an opaque object in either path changes the interference and thus increases the probability of a photon exiting via the dark port. In our realization, the role of the two paths is played by the two circular polarizations and the beam splitters by polarizers as depicted in Figs. 1(a) and 1(b). The first polarizer selects the initial state in the horizontal polarization mode (ε_H), corresponding to an equal superposition of right (ε_R) and left (ε_L) circular polarization modes, $\boldsymbol{E}_{\rm in}=E_0(\varepsilon_R+\varepsilon_L)/\sqrt{2}$. If propagating through a medium with differential absorption for the two opposite circular polarizations and negligible differential dispersion, the state becomes [12]

$$\mathbf{E}_{DC}=E_0\frac{1}{\sqrt{2}}\{e^{-\alpha_R/2}\varepsilon_R+e^{-\alpha_L/2}\varepsilon_L\},\tag{1}$$

where $\alpha_R(\alpha_L)$ is real and indicates the absorption for the right (left) circular polarization. We can rewrite the absorption in terms of differential absorption for the two polarizations defining $\alpha_+=(\alpha_R+\alpha_L)/2$ and $\alpha_-=(\alpha_R-\alpha_L)/2$. The second polarizer separates two orthogonal linear polarization modes, the originally selected ε_H and ε_V. The light intensity exiting at each output of the second polarizer, labeled, respectively, H and V is then

$$I_H=I_0e^{-\alpha_+}\cosh^2\frac{\alpha_-}{2},\tag{2}$$

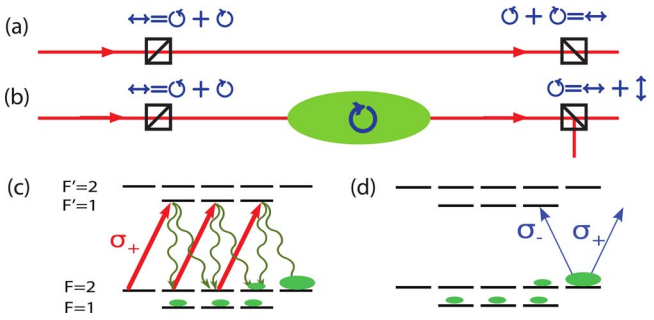

Fig. 1. (Color online) (a) and (b) Scheme of the polarization interferometer, respectively, without and with a dichroic absorber inserted. (c) and (d) Relevant energy levels for pumping and probing of ^{87}Rb together with the induced population distribution. Both pump and probe light are tuned on resonance with the $5^2S_{1/2}(F=2)\rightarrow 5^2P_{1/2}(F'=1)$ transition.

$$I_V = I_0 e^{-\alpha_+} \sinh^2 \frac{\alpha_-}{2}. \quad (3)$$

According to Eq. (3) there is light at the V output only for $\alpha_- \neq 0$.

By optical pumping with circularly polarized light, we generate a circular dichroism feature with a narrow approximately Lorentzian spectrum. The pumping scheme is similar to that of Doppler-free polarization spectroscopy [12,13]. We work with the $5^2S_{1/2}(F=2) \rightarrow 5^2P_{1/2}(F'=1)$ transition of ^{87}Rb at a wavelength of 795 nm. The atomic sample is a hot vapor; therefore the width of the spectral features is dominated by Doppler broadening. As shown in Fig. 1(c), a σ_+ polarized pump drives the atomic population toward the $F=2$, $m_F=1,2$ sublevels. The intensity is chosen such that the resonant velocity group is efficiently pumped ($I \geqslant I_{\mathrm{sat}}$), but other velocity groups experience little pumping effect. This creates a sub-Doppler circular dichroism feature [14,15]. The pump can be tuned to address a narrow velocity class of atoms, determining the central frequency of our filter within the Doppler width of the transition. A similar pumping scheme can be realized for other alkali metals and for different spectroscopic lines, as studied by Harris *et al.* [13].

A schematic of the experimental setup is shown in Fig. 2. The interferometer is composed of a Glan–Thompson (GT) polarizer (extinction ratio 10^5:1) and a Wollaston prism (WP) polarizing beam splitter (extinction ratio 10^5:1 for both outputs). A half-wave plate (HWP_1) is inserted between the two polarizers to balance the interferometer. The two output ports of the WP are coupled into single-mode fibers and detected with two silicon photodiodes (D_H and D_V). The rubidium vapor, a mixture of ^{85}Rb and ^{87}Rb (natural abundance), is contained in a cylindrical glass cell with a diameter of 25.4 mm and a length of 15 cm with windows antireflection coated on both sides. The cell is heated to 65°C, obtaining a pressure of 10^{-5} Torr of rubidium vapor, corresponding to an optical depth of 1.1 on the $F=2 \rightarrow F'=1$ transition. The transmission through the cell for light far detuned from resonance is 95%. A bias magnetic field of the order of 100 mG along the cell axis is generated by a coil. A magnetic shielding chamber made of μ metal reduces the external earth magnetic field to $\leqslant$1 mG. The pump light is provided by an external-cavity diode laser (ECL). For optimal background noise rejection, the pump is directed into the cell counterpropagating with the probe using a large-surface gold-coated mirror with a 3 mm diameter hole drilled at its center. The pump polarization is set to drive the σ_+ transitions by an HWP and a quarter-wave plate (QWP). The angular settings for these wave plates are chosen taking into account also the polarization rotation introduced by reflection on the mirrors. The large pump beam waist (approximately 12 mm) ensures a relatively long average crossing time (>30 μs) for the atoms before reaching the center of the cell and interacting with the probe beam. To achieve velocity-selective pumping neither buffer gas nor a paraffin-coated cell can be used; thus to efficiently polarize the sample, the pump intensity is much greater than the saturation value of the transition $I_{\mathrm{sat}}=1.5$ mW/cm^2. In this way we obtain the measured values of $\alpha_R \approx 5$ and $\alpha_L \approx 0.3$. We use a second ECL as the source of the probe beam. The frequency can be scanned within a range of several gigahertz around the D_1 line of ^{87}Rb. The probe is collimated into the cell with a diameter of 800 μm, and an intensity $\leqslant 0.1\ I_{\mathrm{sat}}$ is used to avoid self-pumping effects on the atoms. Figure 3 shows the spectra collected at the H and V outputs of the interferometer for the pump locked to the $F=2 \rightarrow F'=1$ transition. The transmission is corrected for fiber coupling losses. The V output presents peaks for the $F=2 \rightarrow F'=1$ and $F=2 \rightarrow F'=2$ transitions and a dark background far from resonance. Both peaks are well fitted by Lorentzian distributions in the central part. In the tails of the peaks, the approximation of negligible circular birefringence is not valid anymore. A Gaussian behavior becomes dominant within the Doppler width, while for larger detunings the line shape is Lorentzian again. In Fig. 3, the out-of-band extinction ratio is $\geqslant$35 dB for a probe light detuned by more than 3 GHz, where the effect of the atoms is still appreciable. Further off resonance, the extinction ratio is determined by the quality of the polarizers, their alignment, and the birefringence of the cell

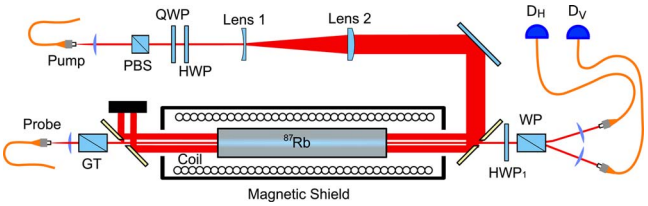

Fig. 2. (Color online) Experimental schematics. Two fiber-coupled external-cavity diodes (not shown) provide probe and pump beams. The probe passes a GT, the Rb vapor cell, and a WP before being collected into single-mode fibers and detected at D_H and D_V. A HWP_1 is used to balance the interferometer. The pump is magnified to a diameter of approximately 25 mm before entering the cell. Gold-coated mirrors with a central 3 mm hole are used to combine the pump and the probe beams with minimal polarization distortion.

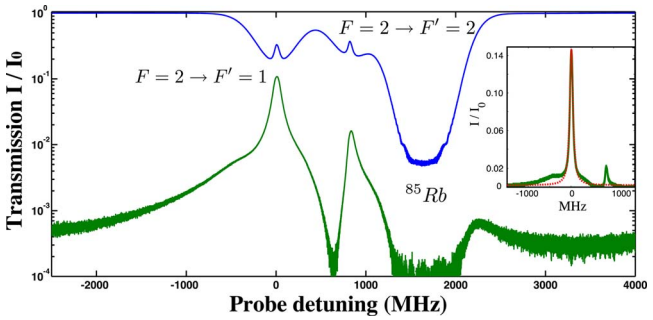

Fig. 3. (Color online) Experimental transmission spectra of the filter (lower curve). The upper curve is a reference saturated spectroscopy signal collected at the H output of the interferometer. Inset, detail of the higher peak and Lorentzian fit (dotted curve).

windows. In a similar setup, an extinction ratio as high as 70 dB was achieved [15].

The maximum observed peak for the $F=2\rightarrow F'=1$ transition is 14.6% of the input light. According to Eq. (3), a higher optical density would permit a higher transmission, but it would also require a higher pump power to maintain a good polarization of the whole atomic sample. Power broadening by the intense pump beam determines a peak width larger than the 6 MHz natural linewidth of the transition; we measured a FWHM of 80 MHz.

The center of the transmission feature can be chosen by tuning the pump frequency within the Doppler profile as shown in Fig. 4(a) (Media 1). Figure 4(b) shows the peak transmission as a function of the pump detuning from the $F=2\rightarrow F'=1$ transition. The maximum transmission is obtained for the pump tuned to the zero-velocity resonance frequency. For light off resonance, the efficiency decreases together with the reduced optical density of the sample following the Doppler profile of the absorption line. A less efficient pumping is also obtained tuning the pump to the $F=2\rightarrow F'=2$ transition.

In conclusion, we have demonstrated a filter for electromagnetic radiation based on an interference technique combined with an appropriate manipulation of the optical properties of an atomic ensemble. We note that the filter could be used with probe modes of various shapes, or with images, provided they are sufficiently collimated. We have measured a peak transmission of 14.6% and a bandwidth $\leqslant$80 MHz, thus attaining a higher transmission and a narrower bandwidth compared to other similar atomic systems [7–9]. We have also demonstrated frequency tuning within the Doppler profile width of the absorption line of rubidium. Moreover, the pumping scheme used can be extended to other spectroscopic lines of other alkali atomic vapors, providing a filter for resonant light in an atomic optics experiment with hot and cold gases.

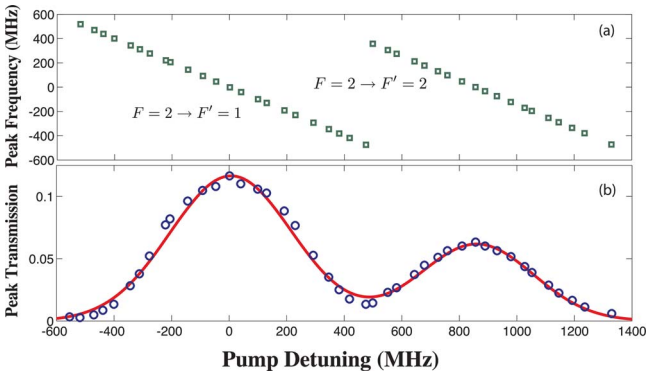

Fig. 4. (Color online) (a) Peak center frequency and (b) maximum transmission as a function of the detuning of the pump from the $F=2\rightarrow F'=1$ transition. Every point corresponds to a frame of Media 1. The transmission is well fitted by the sum of two Gaussian distribution (continuous curve) corresponding to the Doppler absorption profile of the two transitions indicated.

This work was supported by the Spanish Ministerio de Ciencia e Innovación de España through Consolider-Ingenio 2010 Project Quantum Optical Information Technology and MEC project InterFaz Luz-Materia con Conjuntos de Atomos Frios (ref. FIS2008-01051). F. Wolfgramm and A. Predojević are supported by the Commission for Universities and Research of the Department of Innovation, Universities, and Enterprises of the Catalan Government and the European Social Fund.

References

1. T. Junxiong, W. Qingji, L. Yimin, Z. Liang, G. Jianhua, D. Minghao, K. Jiankun, and Z. Lemin, Appl. Opt. **34**, 2619 (1995).
2. C. Fricke-Begemann, M. Alpers, and J. Höffner, Opt. Lett. **27**, 1932 (2002).
3. J. Höffner and C. Fricke-Begemann, Opt. Lett. **30**, 890 (2005).
4. J. S. Neergaard-Nielsen, B. M. Nielsen, H. Takahashi, A. I. Vistnes, and E. S. Polzik, Opt. Express **15**, 7940 (2007).
5. X.-H. Bao, Y. Qian, J. Yang, H. Zhang, Z.-B. Chen, T. Yang, and J.-W. Pan, Phys. Rev. Lett. **101**, 190501 (2008).
6. F. Wolfgramm, X. Xing, A. Cerè, A. Predojević, A. M. Steinberg, and M. W. Mitchell, Opt. Express **16**, 18145 (2008).
7. S. K. Gayen, R. I. Billmers, V. M. Contarino, M. F. Squicciarini, W. J. Scharpf, G. Yang, P. R. Herczfeld, and D. M. Allocca, Opt. Lett. **20**, 1427 (1995).
8. L. D. Turner, V. Karaganov, P. J. O. Teubner, and R. E. Scholten, Opt. Lett. **27**, 500 (2002).
9. Z. He, Y. Zhang, S. Liu, and P. Yuan, Chin. Opt. Lett. **5**, 252 (2007).
10. C. Liu, Z. Dutton, C. Behroozi, and L. V. Hau, Nature **409**, 490 (2001).
11. A. Elitzur and L. Vaidman, Found. Phys. **23**, 987 (1993).
12. C. P. Pearman, C. S. Adams, S. G. Cox, P. F. Griffin, D. A. Smith, and I. G. Hughes, J. Phys. B **35**, 5141 (2002).
13. M. L. Harris, C. S. Adams, S. L. Cornish, I. C. McLeod, E. Tarleton, and I. G. Hughes, Phys. Rev. A **73**, 062509 (2006).
14. W. Happer, Rev. Mod. Phys. **44**, 169 (1972).
15. C. Wieman and T. W. Hänsch, Phys. Rev. Lett. **36**, 1170 (1976).